






## Article

# Evaluation of $V_{TH}$ and $R_{ON}$ Drifts during Switch-Mode Operation in Packaged SiC MOSFETs

Marcello Cioni <sup>1,\*</sup>, Alessandro Bertacchini <sup>2</sup>, Alessandro Mucci <sup>1</sup>, Nicolò Zagni <sup>1</sup>, Giovanni Verzellesi <sup>2</sup>, Paolo Pavan <sup>1</sup> and Alessandro Chini <sup>1</sup>

<sup>1</sup> Dipartimento di Ingegneria “Enzo Ferrari”, University of Modena and Reggio Emilia, Via P. Vivarelli 10, 41125 Modena, Italy; alessandromucci1@gmail.com (A.M.); nicolo.zagni@unimore.it (N.Z.); paolo.pavan@unimore.it (P.P.); alessandro.chini@unimore.it (A.C.)

<sup>2</sup> Dipartimento di Scienze e Metodi dell’Ingegneria, University of Modena and Reggio Emilia, Via Giovanni Amendola 2-Pad. Morselli, 42122 Reggio Emilia, Italy; alessandro.bertacchini@unimore.it (A.B.); giovanni.verzellesi@unimore.it (G.V.)

\* Correspondence: marcello.cioni@unimore.it

**Abstract:** In this paper, we investigate the evolution of threshold voltage ( $V_{TH}$ ) and on-resistance ( $R_{ON}$ ) drifts in the silicon carbide (SiC) power metal-oxide-semiconductor field-effect transistors (MOSFETs) during the switch-mode operation. A novel measurement setup for performing the required on-the-fly characterization is presented and the experimental results, obtained on commercially available TO-247 packaged SiC devices, are reported. Measurements were performed for 1000 s, during which negative  $V_{TH}$  shifts (i.e.,  $V_{TH}$  decrease) and negative  $R_{ON}$  drifts (i.e.,  $R_{ON}$  decrease) were observed. To better understand the origin of these parameter drifts and their possible correlation, measurements were performed for different (i) gate-driving voltage ( $V_{GH}$ ) and (ii) off-state drain voltage ( $V_{PH}$ ). We found that  $V_{TH}$  reduction leads to a current increase, thus yielding  $R_{ON}$  to decrease. This correlation was explained by the  $R_{ON}$  dependence on the overdrive voltage ( $V_{GS}-V_{TH}$ ). We also found that gate-related effects dominate the parameter drifts at low  $V_{PH}$  with no observable recovery, due to the repeated switching of the gate signal required for the parameter monitoring. Conversely, the drain-induced instabilities caused by high  $V_{PH}$  are completely recoverable within 1000 s from the  $V_{PH}$  removal. These results show that the measurement setup is able to discern the gate/drain contributions, clarifying the origin of the observed  $V_{TH}$  and  $R_{ON}$  drifts.

**Keywords:** silicon carbide;  $V_{TH}$  instability;  $R_{ON}$  drift; on-the-fly characterization



**Citation:** Cioni, M.; Bertacchini, A.; Mucci, A.; Zagni, N.; Verzellesi, G.; Pavan, P.; Chini, A. Evaluation of  $V_{TH}$  and  $R_{ON}$  Drifts during Switch-Mode Operation in Packaged SiC MOSFETs. *Electronics* **2021**, *10*, 441. <https://doi.org/10.3390/electronics10040441>

Academic Editor: Gabriel Garcerá

Received: 19 January 2021

Accepted: 5 February 2021

Published: 10 February 2021

**Publisher’s Note:** MDPI stays neutral with regard to jurisdictional claims in published maps and institutional affiliations.



**Copyright:** © 2021 by the authors. Licensee MDPI, Basel, Switzerland. This article is an open access article distributed under the terms and conditions of the Creative Commons Attribution (CC BY) license (<https://creativecommons.org/licenses/by/4.0/>).

## 1. Introduction

Silicon carbide (SiC) is a common technology option for replacing silicon (Si) in power-switching applications that require low switching and conduction losses [1]. Unfortunately, the degradation of key electrical parameters in SiC power devices under repetitive switching stress reduces both device performance and reliability well below specifications [2]. In this scenario, stability issues like threshold voltage ( $V_{TH}$ ) and dynamic on-resistance ( $R_{ON}$ ) drifts are often encountered [3], severely impacting device lifetime and performance. For instance, a positive  $R_{ON}$  drift (i.e., increase) affects the conduction losses within power-switching converters, yielding a considerable efficiency reduction. Similarly, a positive  $V_{TH}$  shift results in a lower current level for a given driving gate voltage ( $V_{GS}$ ) [4,5], whereas negative  $V_{TH}$  variations could impede fully turning off the device, causing unwanted conduction at a large drain bias [6].

Generally, Bias Temperature Instability (BTI) experiments are employed to reveal the mechanisms underlying these issues in SiC technology [7–9]. However, BTI tests can only be used to investigate the effects related to gate bias, neglecting the effects related to the drain bias. To get a more complete picture of the detrimental effects produced by repetitive switching stress [2,10], it is necessary to evaluate the  $V_{TH}$  and  $R_{ON}$  evolution when the

device is driven in realistic operating conditions, i.e., with both gate and drain potential repeatedly switched on and off. To this end, test circuits should be designed to mimic conventional switching conditions in terms of frequency, voltage, and current level. At the same time, these circuits should also extract the parameters of interest (e.g.,  $V_{TH}$  and  $R_{ON}$ ) without affecting device operation. Accordingly, a fast stress measurement approach is needed, in order to cope with switching frequencies in the kHz range [11] and also to limit the delay between the stress and readout [12–14] phases, thus avoiding ambiguous parameter drifts and/or wrong data interpretation. Nevertheless, achieving these goals is challenging for conventional parameter analyzers, especially when characterizing packaged devices with large parasitic capacitances [15]. The development of custom, ad-hoc systems is thus essential to investigate the stability and performance of commercially available state-of-the-art devices.

In this work, we present a novel measurement setup that allows the simultaneous monitoring of both  $V_{TH}$  and  $R_{ON}$  during the conventional switch-mode operation for packaged SiC metal-oxide-semiconductor field-effect transistors (MOSFETs). The measurement is carried out by means of double-pulsed on-the-fly (OTF) characterization, in which the Device Under Test (DUT) is repeatedly switched between a high voltage off-state condition and a low voltage on-state one in the kHz frequency range. To this end, soft-switching conditions are considered (i.e., turn ON and turn OFF transitions are performed at zero current). During OTF measurements, the device  $V_{TH}$  and  $R_{ON}$  are evaluated in order to monitor their drifts over time with a digital sampling oscilloscope (DSO). Since the parameter instabilities could manifest either after a few or several operating cycles [16], it is important to monitor the parameters of interest over several time decades to capture the whole dynamics. Accordingly, the DSO acquisition was triggered at logarithmically spaced time instants in order to avoid memory saturation and loss of accuracy [17]. By applying the proposed measurement method on commercially available devices (i.e., TO-247 vertical SiC MOSFETs), it was possible to test the effectiveness of the setup and to provide a qualitative interpretation of the physical mechanisms leading to the observed  $V_{TH}$  and  $R_{ON}$  drifts. Particularly, negative drifts (i.e., decrease) were observed for both  $V_{TH}$  and  $R_{ON}$ , that can be ascribed to the presence of traps at the SiC/SiO<sub>2</sub> interface [18–20].

The paper is organized as follows. Section 2 describes the custom measurement setup and the adopted design strategies to improve the measurement accuracy. In Section 3, the data collected for tested SiC MOSFETs are presented, highlighting the drift effects on the devices' trans-characteristics. Particularly, we investigated the effect of the bias conditions on the observed drifts, emphasizing the effect of the gate-driving voltage applied in on-state ( $V_{GH}$ ) and of the drain voltage applied during off-state stress ( $V_{PH}$ ). Finally, Section 4 draws the conclusions of the paper.

## 2. Measurement Setup

The simplified schematic of the custom measurement setup is shown in Figure 1. The system was developed starting from the design first presented in [17], with several important modifications as discussed in the following.

The gate driver circuit is responsible for repeatedly switching the DUT ON and OFF and is devoted to the generation of the ramp signal required for the extraction of the  $V_{TH}$  and  $R_{ON}$  values. For performing on-wafer measurements, the usage of a simple waveform generator would be sufficient, thanks to the small parasitic capacitances of the DUTs. However, this solution is not viable for characterizing packaged devices due to the gate-to-source capacitances ( $C_{GS}$ ) in the order of few nF [15]. For this reason, a custom gate driver circuit is required to prevent any distortion of the ramp signal, thus ensuring a fast and accurate  $V_{TH}$  extraction [14].

In off-state conditions, the DUT is stressed with a large drain voltage ( $V_{PH}$ ), provided by a DC power supply, inducing both lateral and vertical trapping [21], while the on-state drain bias voltage ( $V_{PL}$ ) is provided through an isolated DC/DC converter. The drain voltage is pulsed by means of a couple of NMOS ( $M_{PH}$  and  $M_{PL}$  in Figure 1) arranged in a

push–pull configuration, with an additional NMOS device ( $M_{PLL}$ ) inserted for reducing the series resistance during DUT turn-on. A  $0.1 \Omega$  resistor ( $R_{SENSE}$ ) is connected to the DUT's source terminal in order to extract the drain current ( $I_{DS}$ ) while a clamping circuit ( $M_1, R_1, D_1$ ) is connected to the drain terminal of the DUT for improving the measurement accuracy at low voltages. An additional NMOS ( $M_{DSC}$ ) was placed between the DUT's drain terminal and GND in order to force the drain voltage to 0 V. This condition is required for monitoring the parameter recovery after the  $V_{PH}$  removal. The whole setup is controlled by a MicroController Unit (MCU) used for triggering the DSO acquisition with logarithmically spaced time steps [17] and for generating the necessary synchronization signals. Figure 2 illustrates a typical bias scheme for the circuit. Figure 3 shows the time sequence of the trigger signal used to activate the DSO acquisition.

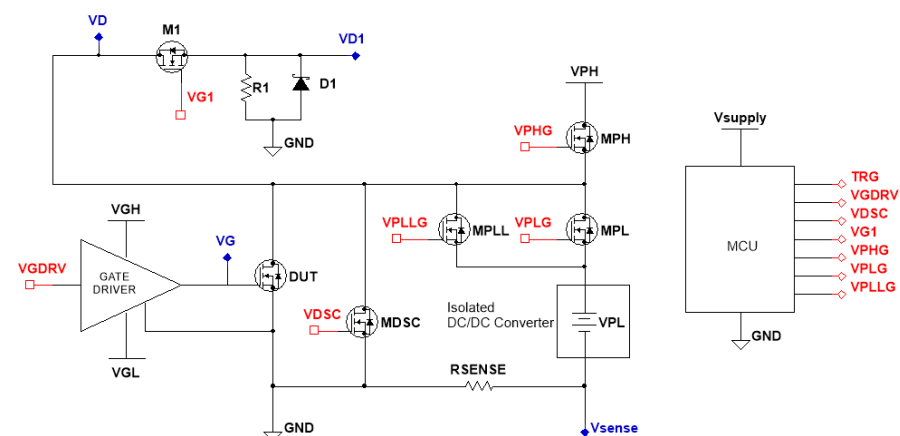


**Figure 1.** Setup schematic. The whole setup is controlled by an MCU used for triggering the DSO acquisition with logarithmic time steps and generating the necessary synchronization signals.

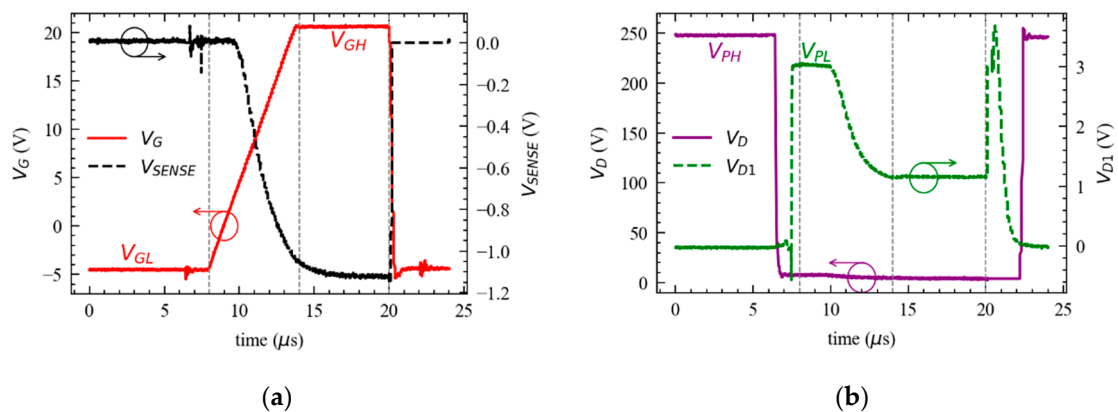


**Figure 2.** (a) Gate voltage ( $V_G$ ) is swept for extracting  $V_{TH}$  and a stable 20 V level is held at the end of the ramp to ensure a stable current and voltage level for a correct  $R_{ON}$  extraction. (b)  $V_D$  is monitored during the off-state stress phase, while  $V_{D1}$  is the signal provided by the clamping circuit ( $M_1, R_1, D_1$ ).

The DSO used in this work was a four-channel PicoScope 5000 Series with 14-bit resolution and a 200 MHz maximum bandwidth. In this study, the rapid block mode was used for data acquisition in order to allow the log-like sampling required for monitoring the drifts over a large time interval.

Measurements were carried out with a  $120 \mu s$  switching period and 10% Duty Cycle, i.e., by applying a gate bias rising from  $-5$  V to 20 V in  $6 \mu s$ , and staying at 20 V for the further  $6 \mu s$  during the low-(drain)-voltage on-state time interval (see Figure 2a). In off-state conditions, a  $V_{PH}$  stress voltage is applied to the DUT, whereas in the on-state  $V_{PL}$  it is set to 3 V (see Figure 2b).  $V_{GL}$  is typically set to  $-5$  V in order to prevent a false

turn-on and ensure the safe operation against voltage spikes on the gate [6]. During the 6  $\mu\text{s}$  rising ramp, the  $I_{\text{DS}}-V_{\text{GS}}$  characteristic is reconstructed, allowing the extraction of the device  $V_{\text{TH}}$  using the extrapolation in the linear regime method [7,22]. To perform a correct  $R_{\text{ON}}$  extraction, at the end of the gate ramp, a stable  $V_{\text{GH}}$  level is held for 6  $\mu\text{s}$  to compute  $R_{\text{ON}}$  as the ratio between the measured  $V_{\text{D1}}$  and  $I_{\text{DS}}$  averaged over the 6  $\mu\text{s}$  range.

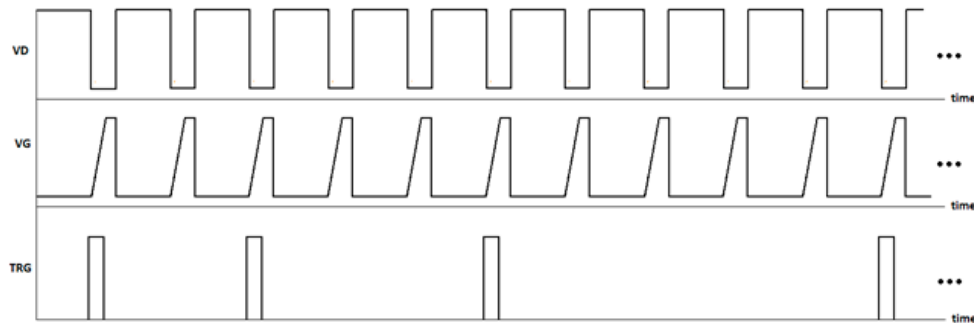


**Figure 3.** Typical measurement sequence: The Device Under Test (DUT) is repeatedly switched ON and OFF at each cycle, but the trigger signal (TRG) is generated only for some predefined periods logarithmically spaced in time. This avoids the DSO's memory saturation, preserving time accuracy.

The chosen  $I_{\text{DS}}-V_{\text{GS}}$  sweep rate represents the best compromise between speed and accuracy, since the short time required for the  $V_{\text{TH}}$  and  $R_{\text{ON}}$  measurement minimizes the fast recovery between stress phases but still provides enough samples for a correct  $I_{\text{DS}}-V_{\text{GS}}$  acquisition.

The DUTs were commercially available TO-247 packaged SiC MOSFETs based on a vertical structure for which a good measurement repeatability was found. Accordingly, we discuss the results obtained on a single device without loss of generality. The fresh  $I_{\text{DS}}-V_{\text{GS}}$  characteristic acquired with the custom setup is shown in Figure 4.

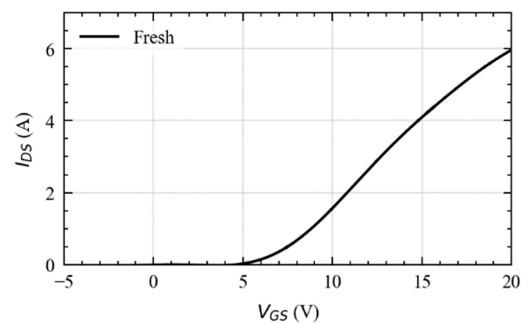


**Figure 4.** Fresh  $I_{\text{DS}}-V_{\text{GS}}$  characteristics for tested silicon carbide (SiC) MOSFET obtained with  $(V_{\text{GL}}; V_{\text{GH}}) = (-5 \text{ V}; 20 \text{ V})$  and  $V_{\text{PL}} = 3 \text{ V}$ .

### 3. Results

In this section, we discuss the results obtained with the OTF characterization system presented in Section 2. The results are shown in terms of  $V_{\text{TH}}$  and  $R_{\text{ON}}$  drifts.

A sequence of no-stress acquisitions (i.e.,  $V_{\text{PH}} = 0 \text{ V}$ ) is performed on fresh devices at the beginning of each characterization and the corresponding  $I_{\text{DS}}-V_{\text{DS}}$  curves were acquired to set a reference value ( $V_{\text{TH0}}$  and  $R_{\text{ON0}}$ ) from which the relative drifts are evaluated. Then, the parameter evolution is monitored for 1000 s.  $\Delta V_{\text{TH}}$  is simply calculated as  $(V_{\text{TH}} - V_{\text{TH0}})$ , whereas the acquired  $R_{\text{ON}}$  values are normalized with respect to the fresh value ( $R_{\text{ON0}}$ ).

### 3.1. $V_{TH}$ and $R_{ON}$ Drifts

The data obtained during the OTF characterization are shown in Figure 5. As we can see in Figure 5a, a significant negative  $V_{TH}$  drift was observed only after several stress cycles (e.g.,  $-0.55$  V at 1000 s). The  $R_{ON}$  parameter evolution is shown in Figure 5b, in which a small benign negative shift of  $\approx -3.5\%$  was observed after 1000 s stress.

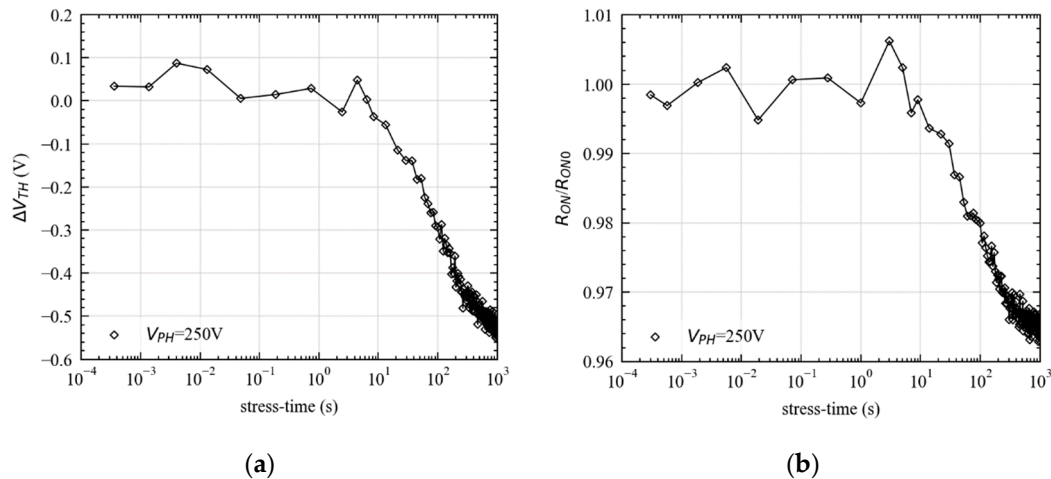


**Figure 5.** Results obtained with  $(V_{GL}; V_{GH}) = (-5$  V; 20 V) and  $(V_{PL}; V_{PH}) = (3$  V; 250 V). (a)  $\Delta V_{TH}$  (i.e.,  $V_{TH} - V_{TH0}$ ). (b) Normalized  $R_{ON}$  variation (i.e.,  $R_{ON}/R_{ON0}$ ).

To gain further insights on the origin of these behaviors, we investigated the trans-characteristics ( $I_{DS} - V_{GS}$ ) evolution during stress. Accordingly, in Figure 6, we report three transfer curves measured at some relevant time instants. That is, the green solid curves, referring to the fresh devices, are used as reference, while the black dotted and red dashed curves correspond to the first ( $\approx 110$   $\mu$ s) and to the last (1000 s) stress period, respectively.

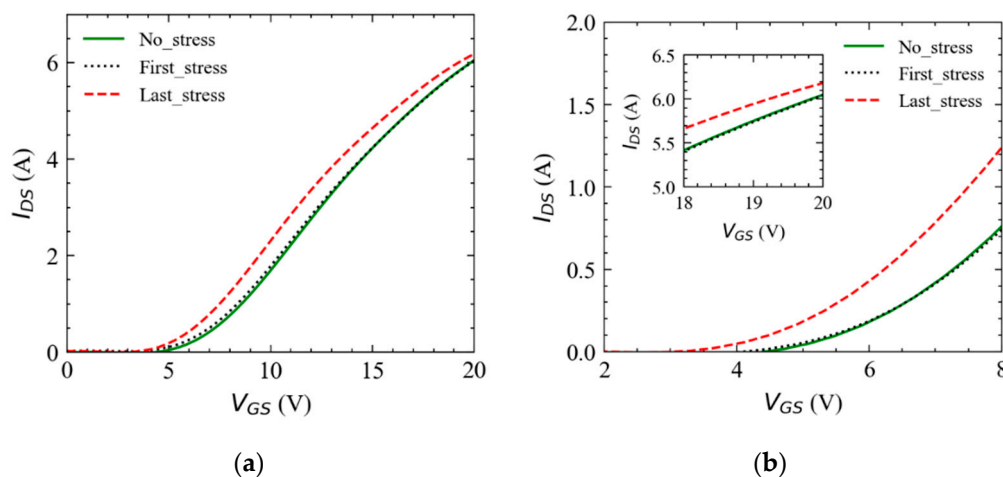


**Figure 6.** (a)  $I_{DS} - V_{GS}$  characteristics from which  $R_{ON}$  and  $V_{TH}$  were extracted. Reported curves were collected for 250 V off-state drain voltage in three different conditions: before stress (green solid lines), after the first stress period of  $\approx 110$   $\mu$ s (black dotted curves), and after 1000 s stress (red dashed curves). (b) Detail of parameters drifts:  $V_{TH}$  moves towards the left after 1000 s of operation. The current increase observed in the triode region (see figure inset) is a signature of decreased  $R_{ON}$ .

The parameter drifts shown in Figure 5 find consistent correspondence with the trans-characteristics drifts of Figure 6. No appreciable drifts were observed after the first stress period on both  $V_{TH}$  and  $R_{ON}$ , whereas non-negligible variations appeared after 1000 s of stress. A considerable triode-current variation (i.e.,  $R_{ON}$  drift) is present in correspondence with the last stress cycle, in which a slight  $I_{DS}$  increase (see inset of Figure 6b) is a signature

of decreased  $R_{ON}$ . The negative  $V_{TH}$  shift observed in Figure 5a is consistent with the  $I_{DS}$  curve shift in Figure 6b after 1000 s. These negative drifts could be potentially explained by the presence of traps at the SiC/SiO<sub>2</sub> interface [18–20] and the long transients observed could be a signature of charge emission dynamics.

### 3.2. Effects of Measurement Conditions on the Parameter Drifts

In order to better understand the mechanism involved in the observed drifts, it is important to know the influence of the measurement conditions on the parameter drifts. To this end, the effects associated to (i) the gate-driving voltage provided in on-state ( $V_{GH}$ ) and (ii) off-state drain voltage ( $V_{PH}$ ) were investigated. With the aim of pursuing a deeper investigation, after 1000 s stress, an additional 1000 s measurement phase was inserted for monitoring the parameter recovery after the  $V_{PH}$  removal. During this additional phase, the  $V_{PH}$  bias is no longer applied to the DUT and the drain voltage in the off-state condition is set to 0 V. On the other hand, the same gate ramp ( $V_{GL}$ ;  $V_{GH}$ ) and low drain voltage ( $V_{PL}$ ) are provided to the DUT for extracting  $V_{TH}$  and measuring  $R_{ON}$  in the triode region.

To highlight the  $V_{GH}$  effect on the observed drifts, the characterization was performed by ramping the gate voltage from  $-5$  V to three different  $V_{GH}$  levels (15 V, 17.5 V, and 20 V), whereas the  $V_{PH}$  voltage was fixed to 100 V. The results obtained for the  $V_{TH}$  and  $R_{ON}$  parameters are shown in Figures 7 and 8, respectively.

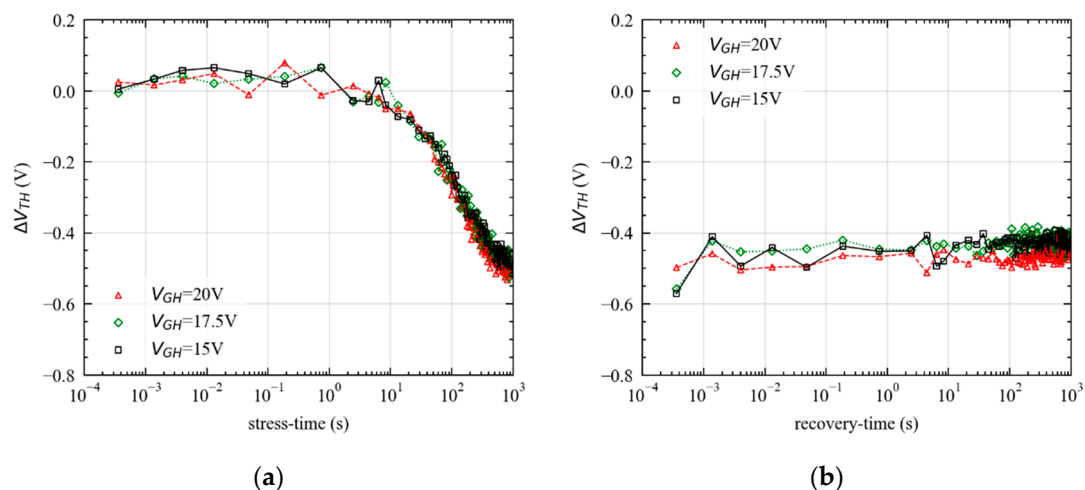


**Figure 7.** (a) Effect of gate voltage level ( $V_{GH}$ ) on the  $V_{TH}$  drift during the stress with  $V_{PH} = 100$  V. (b) Monitored  $V_{TH}$  recovery at different  $V_{GH}$  levels (15 V, 17.5 V, and 20 V) with  $V_{PH} = 100$  V.

The transients observed for both  $V_{TH}$  and  $R_{ON}$  during the stress phase present similar time constants, suggesting a possible correlation between the two phenomena. Particularly, the observed negative  $V_{TH}$  drift should lead to an increase in device conductivity (at a fixed driving  $V_{GH}$ ), thus yielding a  $R_{ON}$  reduction. The observed  $R_{ON}$  transient (Figure 8a) could thus be a directly correlated to the  $V_{TH}$  ones (Figure 7a), indicating the presence of a single underlying mechanism.

However, a different  $V_{GH}$  effect was observed for  $V_{TH}$  and  $R_{ON}$  transients during the stress phase. As shown in Figure 7a, the  $V_{TH}$  transients are not affected by the applied  $V_{GH}$ , while a reduction in the  $R_{ON}$  drift is observed for higher  $V_{GH}$ . This can actually be ascribed to the fact that at higher  $V_{GH}$ , the device transconductance ( $g_m$ ) degrades [23], yielding a negligible impact on the overdrive voltage (i.e.,  $V_{GS}-V_{TH}$ ) variations on the device current and, consequently, on  $R_{ON}$ . On the other hand, at lower  $V_{GH}$ , variations in the  $V_{TH}$  affect the device current (i.e.,  $R_{ON}$ ), due to a less degraded  $g_m$  [23]. Accordingly, the  $R_{ON}$  variation increases with decreasing  $V_{GH}$  from 20 V to 15 V (see Figure 8a), even though the associated  $V_{TH}$  transients present negligible differences (i.e., the  $V_{TH}$  drift is the same). Concerning the recovery phase (see Figures 7b and 8b), both  $V_{TH}$  and  $R_{ON}$  drifts are unrecoverable in the considered time interval (i.e., 1000 s), independently on

the applied  $V_{GH}$  level. This observation can be explained in two ways. (i) The recovery transients could present time constants longer than 1000 s, thus making the employed time window insufficient for observing them; (ii) the applied  $V_{PH}$  stress (i.e., 100 V) does not affect the parameter drifts, and the observed instabilities can be totally ascribed to the gate switching applied during the OTF measurement. In fact, monitoring the device parameters in the recovery phase requires the gate voltage to be repeatedly switched from negative to positive and vice versa. As a consequence, the corresponding stress cannot be removed, making the second hypothesis more likely. To prove this point, the drain bias should be completely removed from the stress phase ( $V_{PH} = 0$  V), thus monitoring the DUT behavior when just the  $V_{GS}$  stress is applied. Clearly, the results obtained with  $V_{PH} = 0$  V do not mimic a real operative condition but are nonetheless useful to clarify the origin of the observed drifts.

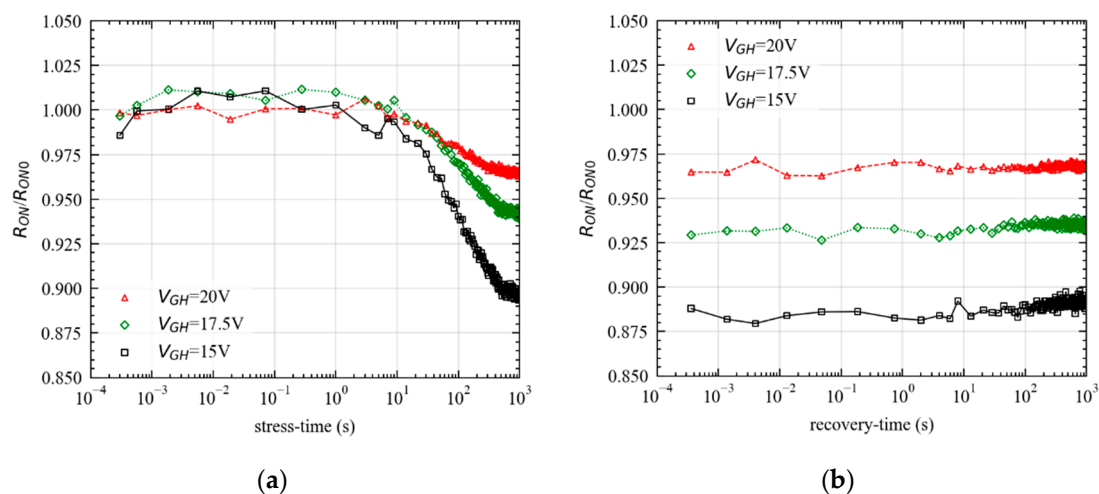


**Figure 8.** (a) Effect of gate voltage level ( $V_{GH}$ ) on the  $R_{ON}$  drift during stress with  $V_{PH} = 100$  V. At an increasing  $V_{GH}$ , the  $R_{ON}$  transient amplitude decreases. (b) Monitored  $R_{ON}$  recovery at different  $V_{GH}$  levels (15 V, 17.5 V, and 20 V) with  $V_{PH} = 100$  V.

The results obtained with  $V_{PH} = 0$  V are shown in Figure 9, in which the transients measured during the stress phase are compared with those obtained for  $V_{PH} = 100$  V.

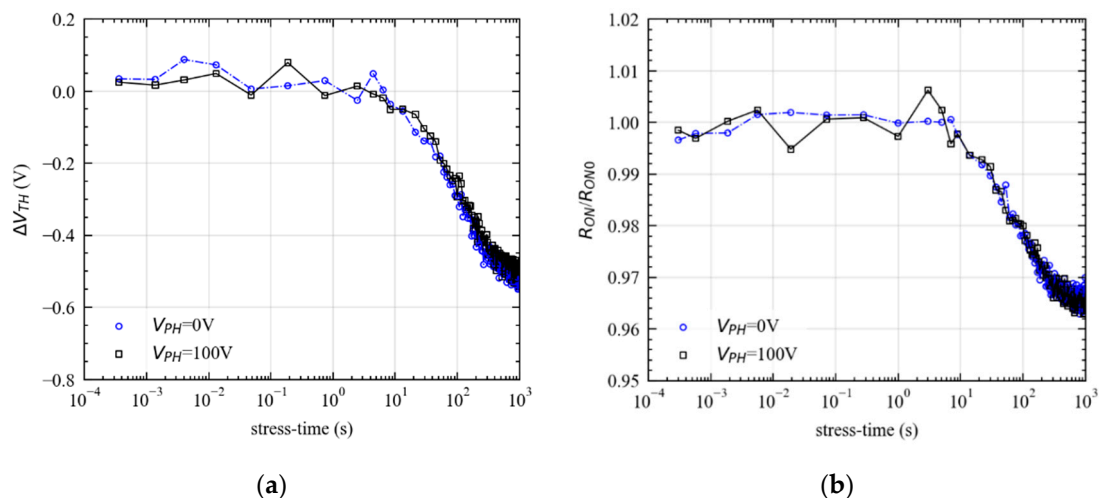


**Figure 9.** Comparison between (a)  $V_{TH}$  and (b)  $R_{ON}$  drift obtained with  $V_{PH} = 0$  V and  $V_{PH} = 100$  V.

The results shown in Figure 9 confirm our hypothesis, since no appreciable variation between the drifts measured with  $V_{PH} = 0$  V and  $V_{PH} = 100$  V was found, yielding nicely

overlapped transients. Accordingly, the observed drifts can be totally ascribed to the driving  $V_{GS}$ , at least for relatively low  $V_{PH}$  (i.e., 100 V). This result is consistent with the vertical structure presented by tested devices. In fact, the influence of the drain voltage on interface states is limited by the physical distance between the oxide and the drain contact, while the gate bias plays a major role on the  $V_{TH}$  stability [7–9]. However, thanks to the large breakdown voltage of SiC devices, the drain voltage applied in the off-state could be significantly higher than 100 V during a typical switching operation; thus, the complete absence of drain-induced instabilities cannot be ruled out. Accordingly, the  $V_{PH}$  role has to be studied for sufficiently high stress voltages to observe the corresponding effect.

We now investigate the  $V_{TH}$  and  $R_{ON}$  drifts at higher stress voltages ( $V_{PH}$ ). To this end, it is important to keep the driving  $V_{GL}$  and  $V_{GH}$  constant in order to discern the gate/drain contributions. Accordingly, a gate voltage between  $-5$  V and  $20$  V was applied to the DUT, consistently with the waveforms reported in Figure 2, while three different  $V_{PH}$  levels were considered (100 V, 250 V, and 500 V). A non-negligible  $V_{PH}$  effect is observed on the  $V_{TH}$  transients (Figure 10), whereas the corresponding  $R_{ON}$  drifts present a weak dependence on the applied  $V_{PH}$  (see Figure 11).

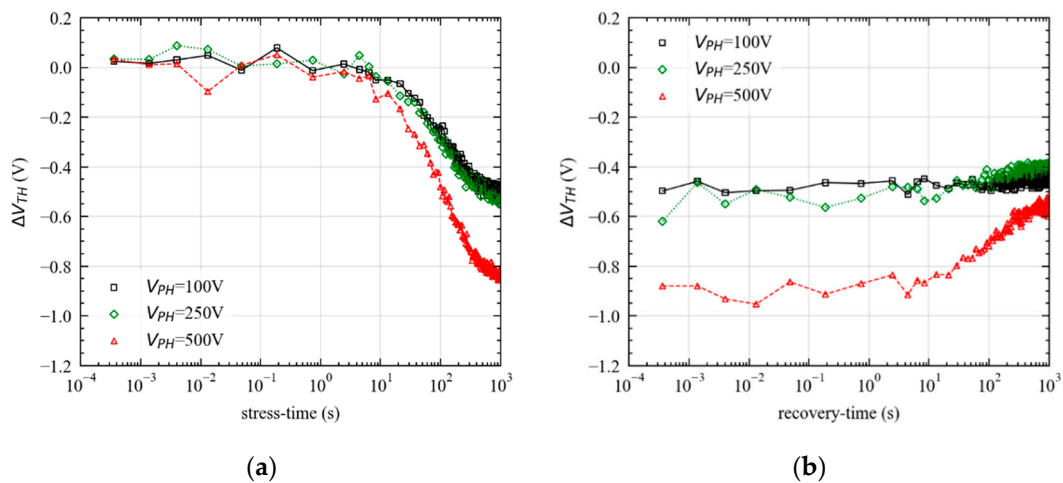


**Figure 10.** (a) Effect of drain off-state stress voltage (100 V, 250 V, and 500 V) on the  $V_{TH}$  drift with  $V_{GH} = 20$  V. (b) Monitored  $V_{TH}$  recovery after  $V_{PH}$  removal ( $V_{GH} = 20$  V).

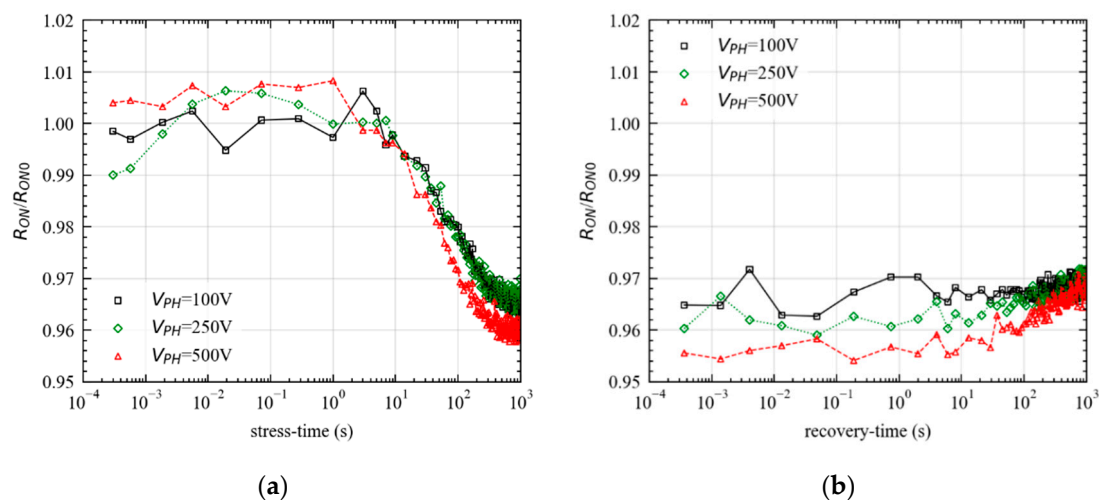


**Figure 11.** (a) Effect of drain off-state stress voltage (100 V, 250 V, and 500 V) on the  $R_{ON}$  drift during the stress with  $V_{GH} = 20$  V. At an increasing stress voltage, the  $R_{ON}$  drift retained after 1000 s does not change significantly. (b) Monitored  $R_{ON}$  recovery for different drain stress voltages.



Negligible differences were observed on the  $V_{TH}$  transients measured at 100 V and 250 V, whereas the negative  $V_{TH}$  shift is more pronounced at  $V_{PH} = 500$  V (Figure 10a), indicating that the off-state stress voltage plays a role to some extent. Interestingly, this additional drift is recoverable within 1000 s from the  $V_{PH}$  removal (see Figure 10b), indicating that negative BTI (NBTI) effects are non-permanent and are enhanced by high  $V_{PH}$  values. The fact that stress and recovery transients have similar time constants suggests that both mechanisms are governed by two similar and opposite slow processes. Moreover, no recovery was observed for  $V_{PH} = 100$  V and  $V_{PH} = 250$  V, confirming that lower off-state stress voltages do not produce any additional instability with respect to that induced by the gate potential. On the other hand, as shown in Figure 11, the slow  $R_{ON}$  transients observed in the range between 1 s and 1000 s present negligible  $V_{PH}$  dependence and just a weak recovery appears at  $V_{PH} = 500$  V (at least within 1000 s from the stress removal, as discussed in Section 3.1). This result is consistent with the  $V_{GH}$  dependence previously investigated, indicating that the large gate bias applied in this phase (i.e.,  $V_{GH} = 20$  V) makes the device current less sensitive to the  $V_{TH}$  variations. In fact, the maximum  $R_{ON}$  dynamics was observed at  $V_{GH} = 15$  V (see Figure 7a), indicating that this condition is optimal to highlight the  $V_{PH}$  effect even on the  $R_{ON}$  parameter. Accordingly, a new set of measurements was taken for a gate voltage ranging between  $V_{GL} = -5$  V and  $V_{GH} = 15$  V, exploring the same  $V_{PH}$  levels used previously (100 V, 250 V, and 500 V). The corresponding  $V_{TH}$  and  $R_{ON}$  drifts are reported in Figures 12 and 13, respectively.

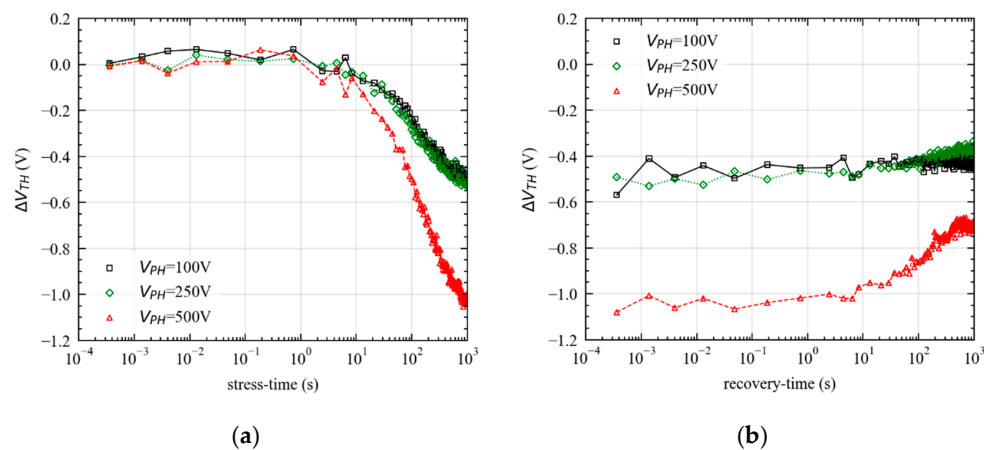


**Figure 12.** (a) Effect of drain off-state stress voltage (100 V, 250 V, and 500 V) on the  $V_{TH}$  drift during the stress with  $V_{GH} = 15$  V. At  $V_{PH} = 500$  V, the negative  $V_{TH}$  drift retained after 1000 s increases. (b) Monitored  $V_{TH}$  recovery at different drain stress voltages.

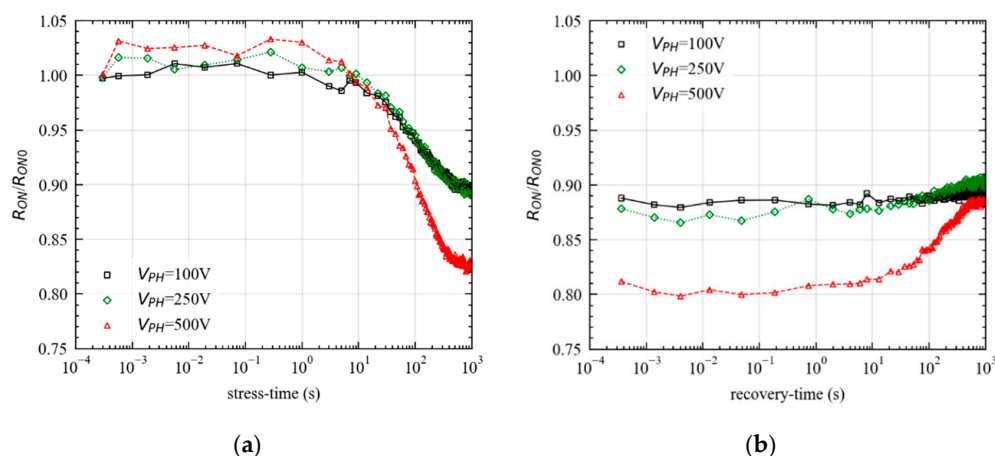


**Figure 13.** (a) Effect of drain off-state stress voltage on the  $R_{ON}$  drift during the stress with  $V_{GH} = 15$  V. The  $R_{ON}$  drift retained after 1000 s increases for  $V_{PH} = 500$  V. (b) Monitored  $R_{ON}$  recovery at different drain stress voltages (100 V, 250 V, and 500 V) with  $V_{GH} = 15$  V.

Once again, the negative  $V_{TH}$  shift observed at  $V_{PH} = 500$  V is stronger with respect to that measured at lower  $V_{PH}$  (Figure 12a). At the same time, the  $R_{ON}$  drift clearly changes from  $-10\%$  to  $-17\%$  while passing from 250 V to 500 V, showing the same  $V_{PH}$  dependence observed on  $V_{TH}$  (compare Figures 12a and 13a). The fact that similar trends were observed on both  $V_{TH}$  and  $R_{ON}$  degradation confirms that the observed instabilities share the same origin. Particularly, the  $R_{ON}$  drift is a direct consequence of the  $V_{TH}$  one, since at  $V_{GH} = 15$  V, the less degraded  $g_m$  [23] makes the device current (i.e.,  $R_{ON}$ ) highly sensitive on the overdrive voltage (i.e.,  $V_{GH} - V_{TH}$ ). Accordingly, the significant impact of the drain stress voltage observed on  $V_{TH}$  yields an additional  $R_{ON}$  drift at  $V_{PH} = 500$  V, whereas a negligible effect is observed at 100 V and 250 V.

Further evidence of the  $V_{PH}$  role is given by the partial recovery observed after 500 V stress. Almost no recovery was observed after the stress performed at 100 V and 250 V, whereas the recovery transients appear for both  $R_{ON}$  and  $V_{TH}$  at 500 V. In fact, after the  $V_{PH}$  removal, the drain-induced instabilities can be recovered, whereas the gate-induced ones are still present, yielding a residual drift in  $V_{TH}$  and  $R_{ON}$ . Accordingly, the recovery monitoring can be used to isolate the drain-induced instabilities from the gate-related ones, whereas the effect of the gate-driving voltage can be observed by reducing (or by possibly removing)  $V_{PH}$ .

#### 4. Conclusions and Recommendations

The developed measurement technique is able to highlight  $V_{TH}$  and  $R_{ON}$  drifts in packaged SiC power devices. The observed slow negative  $V_{TH}$  shift was associated with the presence of traps at the SiC–SiO<sub>2</sub> interface. A direct correlation between  $V_{TH}$  and  $R_{ON}$  drifts was first speculated and then verified. To this end, the impacts of the gate-driving voltage ( $V_{GH}$ ) and of the off-state stress drain voltage ( $V_{PH}$ ) were separately investigated. At a relatively low  $V_{PH}$  (i.e., 100 V), the drifts can be totally ascribed to the repeated switching of the gate signal, whereas the  $V_{PH}$  influence could be observed only at 500 V. This result is consistent with the vertical structure of tested devices, for which the gate potential is expected to mainly affect the dynamics of traps at the oxide–semiconductor interface. In order to observe drain-related effects in vertical devices, it is thus recommended to apply a large off-state stress voltage ( $V_{PH}$ ), which was limited to 500 V in this study. The outcomes obtained with the developed system are instrumental to reveal the mechanisms limiting device stability and performance, by discerning the gate/drain contribution on the parameter degradation. To get a better insight into gate-related effects, in future works, we will investigate other bias combinations, and we will study the effect of the negative gate voltage applied in the off-state ( $V_{GL}$ ). Moreover, the capabilities of the designed setup will be further enhanced by including hard-switching characterization, which will be used to highlight the effect of the transitions when SiC devices are driven in more severe switching conditions.

**Author Contributions:** Conceptualization, M.C. and A.C.; methodology, A.C.; software, M.C., A.M. and A.B.; validation, M.C.; formal analysis, M.C.; investigation, M.C.; resources, A.C.; data curation, M.C.; writing—original draft preparation, M.C.; writing—review and editing, N.Z., G.V., P.P. and A.C.; visualization, M.C.; supervision, A.C.; project administration, A.C.; funding acquisition, A.C. All authors have read and agreed to the published version of the manuscript.

**Funding:** This research was partially funded by the EC project REACTION (G.A. 783158) via the IUNET Consortium.

**Data Availability Statement:** The data presented in this study are available on request from the corresponding author.

**Acknowledgments:** The authors would like to thank Luca Selmi from the University of Modena and Reggio Emilia for the fruitful discussion.

**Conflicts of Interest:** The authors declare no conflict of interest.

## References

1. Kimoto, T.; Cooper, J.A. *Fundamentals of Silicon Carbide Technology: Growth, Characterization, Devices and Applications*; Wiley: Singapore, 2014.
2. Ouaida, R.; Berthou, M.; Leon, J.; Perpina, X.; Oge, S.; Brosselard, P.; Joubert, C. Gate oxide degradation of SiC MOSFET in switching conditions. *IEEE Electron. Device Lett.* **2014**, *35*, 1284–1286. [[CrossRef](#)]
3. Wei, J.; Liu, S.; Lou, R.; Tang, L.; Ye, R.; Zhang, L.; Zhang, X.; Sun, W.; Bai, S. Investigation on the Degradation Mechanism for SiC Power MOSFETs under Repetitive Switching Stress. *IEEE J. Emerg. Sel. Top. Power Electron.* **2019**, *1*. [[CrossRef](#)]
4. Yang, S.; Lu, T.; Liu, S.; Wang, H.; Liu, C.; Chen, K.J. Impact of  $V_{th}$  shift on  $R_{on}$  in E/D-mode GaN-on-Si power transistors: Role of dynamic stress and gate overdrive. In Proceedings of the 2016 28th International Symposium on Power Semiconductor Devices and ICs (ISPSD), Prague, Czech Republic, 12–16 June 2016; pp. 263–266.
5. Guevara, E.; Herrera-Pérez, V.; Rocha, C.; Guerrero, K. Threshold voltage degradation for n-channel 4H-SiC power MOSFETs'. *JLPEA* **2020**, *10*, 3. [[CrossRef](#)]
6. Hua, M.; Wei, J.; Bao, Q.; Zhang, Z.; Zheng, Z.; Chen, K.J. Dependence of  $V_{th}$  stability on gate-bias under reverse-bias stress in E-mode GaN MIS-FET. *IEEE Electron Device Lett.* **2018**, *39*, 413–416. [[CrossRef](#)]
7. Gurfinkel, M.; Suehle, J.; Bernstein, J.; Shapira, Y.; Lelis, A.; Habersat, D.B.; Goldsman, N. Ultra-fast measurements of  $V_{th}$  instability in SiC MOSFETs due to positive and negative constant bias stress. In Proceedings of the 2006 IEEE International Integrated Reliability Workshop Final Report, South Lake Tahoe, CA, USA, 16–19 October 2006; pp. 49–53.
8. Lelis, A.J.; Green, R.; Habersat, D.B.; Goldsman, N. Effect of threshold-voltage instability on SiC DMOSFET reliability. In Proceedings of the 2008 IEEE International Integrated Reliability Workshop Final Report, South lake Tahoe, CA, USA, 12–16 October 2008; pp. 72–76.
9. Ghosh, A.; Hao, J.; Cook, M.; Kendrick, C.; Suliman, S.A.; Hall, G.D. Studies of bias temperature instabilities in 4H-SiC DMOSFETs. In Proceedings of the 2020 IEEE International Reliability Physics Symposium (IRPS), Dallas, TX, USA, 28 April 2020; pp. 1–4.
10. Schrock, J.A.; Pushpakaran, B.N.; Bilbao, A.V.; Ray, W.B.; Hirsch, E.A.; Kelley, M.D.; Holt, S.L.; Bayne, S.B. Failure analysis of 1200-V/150-A SiC MOSFET under repetitive pulsed overcurrent conditions. *IEEE Trans. Power Electron.* **2016**, *31*, 1816–1821. [[CrossRef](#)]
11. Calderon-Lopez, G.; Forsyth, A. High power density DC-DC converter with SiC MOSFETs for electric vehicles. In Proceedings of the 7th IET International Conference on Power Electronics, Machines and Drives (PEMD 2014); Institution of Engineering and Technology, Manchester, UK, 8–10 April 2014; p. 1.
12. Habersat, D.B.; Lelis, A.J.; Green, R. Measurement considerations for evaluating BTI effects in SiC MOSFETs. *Microelectron. Reliab.* **2018**, *81*, 121–126. [[CrossRef](#)]
13. Berens, J.; Weger, M.; Pobegen, G.; Aichinger, T.; Rescher, G.; Schleich, C.; Grasser, T. Similarities and differences of BTI in SiC and Si power MOSFETs. In Proceedings of the 2020 IEEE International Reliability Physics Symposium (IRPS), Dallas, TX, USA, 28 April 2020; pp. 1–7.
14. Lelis, A.J.; Habersat, D.; Green, R.; Ogunniyi, A.; Gurfinkel, M.; Suehle, J.; Goldsman, N. Time dependence of bias-stress-induced SiC MOSFET threshold-voltage instability measurements. *IEEE Trans. Electron Devices* **2008**, *55*, 1835–1840. [[CrossRef](#)]
15. Sheng, H.; Chen, Z.; Wang, F.; Millner, A.R. Investigation of 1.2 kV SiC MOSFET for high frequency high power applications. In Proceedings of the 2010 Twenty-Fifth Annual IEEE Applied Power Electronics Conference and Exposition (APEC), Palm Springs, CA, USA, 21–25 February 2010; pp. 1572–1577.
16. Mori, Y.; Hisamoto, D.; Tega, N.; Matsumura, M.; Yoshimoto, H.; Shima, A.; Shimamoto, Y. Effects of interface properties in SiC MOSFETs on reliability. In Proceedings of the 2015 IEEE 22nd International Symposium on the Physical and Failure Analysis of Integrated Circuits, Hsinchu, Taiwan, 29 June–2 July 2015; pp. 68–71.
17. Chini, A.; Iucolano, F. Evolution of on-resistance ( $R_{on}$ ) and threshold voltage ( $V_{th}$ ) in GaN HEMTs during switch-mode operation. *Mater. Sci. Semicond. Process.* **2018**, *78*, 127–131. [[CrossRef](#)]
18. Kwietniewski, N.; Piotrowski, T.; Gutt, T.; Piotrowska, A.; Gołaszewska, K.; Rzdokiewicz, W.; Sochacki, M.; Szmiedt, J. Oxidation process of SiC by RTP technique. *Mater. Sci. Forum* **2009**, *615–617*, 529–532. [[CrossRef](#)]
19. Lelis, A.J.; Green, R.; Habersat, D.B.; El, M. Basic mechanisms of threshold-voltage instability and implications for reliability testing of SiC MOSFETs. *IEEE Trans. Electron. Devices* **2015**, *62*, 316–323. [[CrossRef](#)]
20. Lelis, A.J.; Green, R.; Habersat, D.B. SiC MOSFET threshold-stability issues. *Mater. Sci. Semicond. Process.* **2018**, *78*, 32–37. [[CrossRef](#)]
21. Meneghini, M.; Vanmeerbeek, P.; Silvestri, R.; Dalcanale, S.; Banerjee, A.; Bisi, D.; Zaroni, G.; Meneghesso, G.; Moens, P. Temperature-dependent dynamic  $R_{on}$  in GaN-bMIS-HEMTs: Role of surface traps and buffer leakage. *IEEE Trans. Electron. Devices* **2015**, *62*, 782–787. [[CrossRef](#)]
22. Ortiz-Conde, A.; Sánchez, F.G.; Liou, J.; Cerdeira, A.; Estrada, M.; Yue, Y. A review of recent MOSFET threshold voltage extraction methods. *Microelectron. Reliab.* **2002**, *42*, 583–596. [[CrossRef](#)]
23. Islam, M.S.; Akanda, R.K.; Anwar, S.; Shahriar, A. Analysis of resistances and transconductance of SiC MESFET considering fabrication parameters and mobility as a function of temperature. In Proceedings of the International Conference on Electrical & Computer Engineering (ICECE 2010), Dhaka, Bangladesh, 18–20 December 2010; pp. 5–8.